Investigation of effect of using organic surfactant in structural properties of $CuFe_2O_4$ nanoparticles

Mahnaz Kamel Attar Kar [a], Faranak Manteghi [a*], Reza Fazaeli [b]

[a] Department of Chemistry, Iran University of Science and Technology, Tehran, Iran

[b] Department of Chemistry, Faculty of Sciences, South Tehran branch, Islamic Azad University, Tehran, Iran

$CuFe_2O_4$ have been widely investigated and used in variety of applications such as magnetic material, anode material, catalyst, and so on, because of their attractive magnetic, electronic, thermal and catalytic properties.

Among methods to synthesize nanoferrites, the combustion synthesis is an easy, safe, rapid and economic method used to synthesise various oxides or to prepare multi-component ceramics. The process is based on a rapid redox reaction between a fuel (urea, citric acid, glycine, etc.) and oxidisers (generally metal nitrates), which starts under a moderated heating. This exothermic reaction can produce some fumes and/or a flame.

Applying surfactants, which are composed from molecules along with sol–gel method can improve the properties of the synthesized powders. In the presence of surfactant, surface tension of solution is reduced and this facilitates nucleation and formation of the new phases. The formation of reverse micelles in gel can be effective in controlling the particles growth and the distance between particles. It has been found that the surfactant prevents the agglomeration of the ferrite nanoparticles.

In this present study, the sol–gel auto-combustion method is applied for synthesizing the $CuFe_2O_4$, $CuFe_2O_4$/CTAB and $CuFe_2O_4$/SDS nanocomposite, using nickel nitrate, iron nitrate, ammonia, citric acid and CTAB and SDS as surfactant. The nanoparticles were characterized by XRD, SEM and FT-IR. Powder XRD analysis and FT-IR spectroscopy confirmed formation of $CuFe_2O_4$ spinel phase. SEM images show the effect of surfactants on morphology of nanoparticles.

1. Introduction

$CuFe_2O_4$ have been widely investigated and used in variety of applications such as magnetic material, anode material, catalyst, and so on, because of their attractive magnetic, electronic, thermal and catalytic properties [1]. $CuFe_2O_4$ is known to exist in tetragonal and cubic structures. Under slow cooling Cu-ferrite crystallizes in a tetragonal structure with lattice parameter ratio c/a of about 1.06. Tetragonal phase of Cu-ferrite has inverse spinel structure with almost all Cu^{2+} ions occupying octahedral sublattice, whereas Fe^{3+} ions divide equally between the tetrahedral and octahedral sublattices. The tetragonal structure is stable at room temperature and transforms to cubic phase only at a temperature of 360∘C and above due to Jahn–Teller distortion. The distortion is directly related to the magnetic properties. The cubic structure possesses a larger magnetic moment than that of the tetragonal one, because there are

more cubic ions (Cu^{2+}) at tetrahedral sites in cubic structure as compared to that in the case of tetragonal structure [2].

Various methods are used to synthesize ferrite nanoparticles, such as: combustion, mechano-chemical method, redox process, forced hydrolysis, co-precipitation, sol–gel, hydrothermal, polymer combustion method (PC), solid state method (SS), micro-emulsion, sonochemical, electrochemical and thermal decomposition method [3-11]. Among methods to synthesize nanocrystalline $CuFe_2O_4$, combustion method seems to be one of the facile and one step methods, since it allows the preparation of nanocrystalline $CuFe_2O_4$ with an equiaxial shape and narrow size distribution [12].

Applying surfactants, which are composed from molecules, contains of hydrophilic head and hydrophobic tail, along with sol–gel method can improve the properties of the synthesized powders. In the presence of surfactant, surface tension of solution is reduced and this facilitates nucleation and formation of the new phases. The formation of reverse micelles in gel can be effective in controlling the particles growth and the distance between particles. Depending on surfactant's head electric charge, surfactants can be divided into three categories: cationic, anionic and nonionic [13].

In this present study, the sol–gel auto-combustion method is applied for synthesizing the $CuFe_2O_4$, $CuFe_2O_4/CTAB$ and $CuFe_2O_4/SDS$ nanocomposite, using copper nitrate, iron nitrate, ammonia, citric acid and CTAB and SDS as surfactant.

2. Experimental

The starting materials for the synthesis of $CuFe_2O_4$, $CuFe_2O_4/CTAB$ and $CuFe_2O_4/SDS$ are $Cu(NO_3)_2·6H_2O$, $Fe(NO_3)_3·9H_2O$, ammonia (30%), citric acid monohydrate (98%) (CA), CTAB and SDS as surfactant. The required amount of metal nitrates and citric acid are taken so as to have a molar ratio of 1:1 and dissolved in 100 mL of deionized water. A required amount of ammonia is added into the solution in order to modify the pH value to about 7. The stoichiometric amount of surfactant was dissolved in minimum amount of water then added to the above solution. Dehydration of the solution was then done on a hotplate at 80◦C until a gel forms. Dry gels were heated in air to about 300◦C to invoke combustion. During combustion large amounts of gas were given off and a lightweight massive powder formed quickly. The resulting "precursor" powder was lightly ground by hand, as well as calcined at 800◦C for 2 h in a furnace to remove any organic rest [14, 15].

3. Results and discussion

3.1 XRD analysis

X-ray diffraction patterns of $CuFe_2O_4$, $CuFe_2O_4$ using CTAB as surfactant and $CuFe_2O_4$ using SDS as surfactant are shown in Figure 1. X-ray diffraction confirms the formation of single-phase (fcc) spinel structure for samples. The XRD pattern was compared and indexed using ICDD card no. (06–0545).
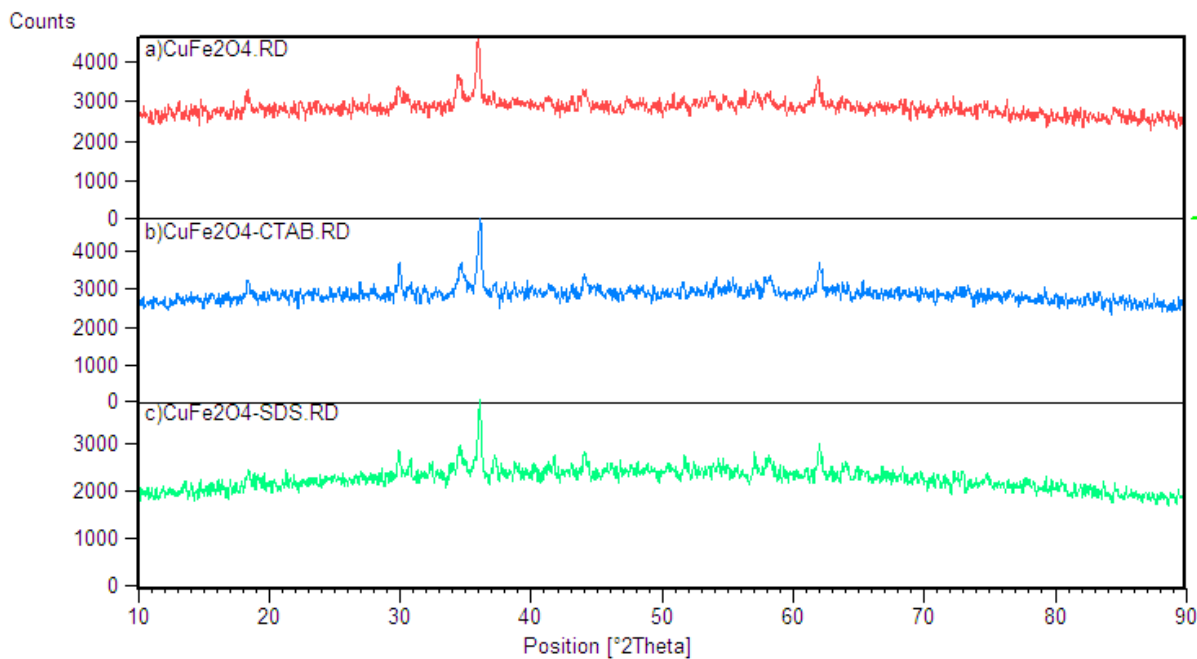
Fig. 1. XRD patterns: a) CuFe$_2$O$_4$, b) CuFe$_2$O$_4$/CTAB and c) CuFe$_2$O$_4$/SDS.

3.2 FT-IR analysis

Figure 2 shows the FT-IR spectrum of the CuFe$_2$O$_4$ powders. The characteristic peaks of tetrahedral and octahedral complexes could be observed at 577 cm^{-1} and 464 cm^{-1}. It is clear that the normal mode of vibration of tetrahedral cluster is higher and normal mode of vibration of octahedral cluster is shorter. The tetrahedral cluster has shorter bond lengths and the octahedral cluster has longer bond lengths [14].
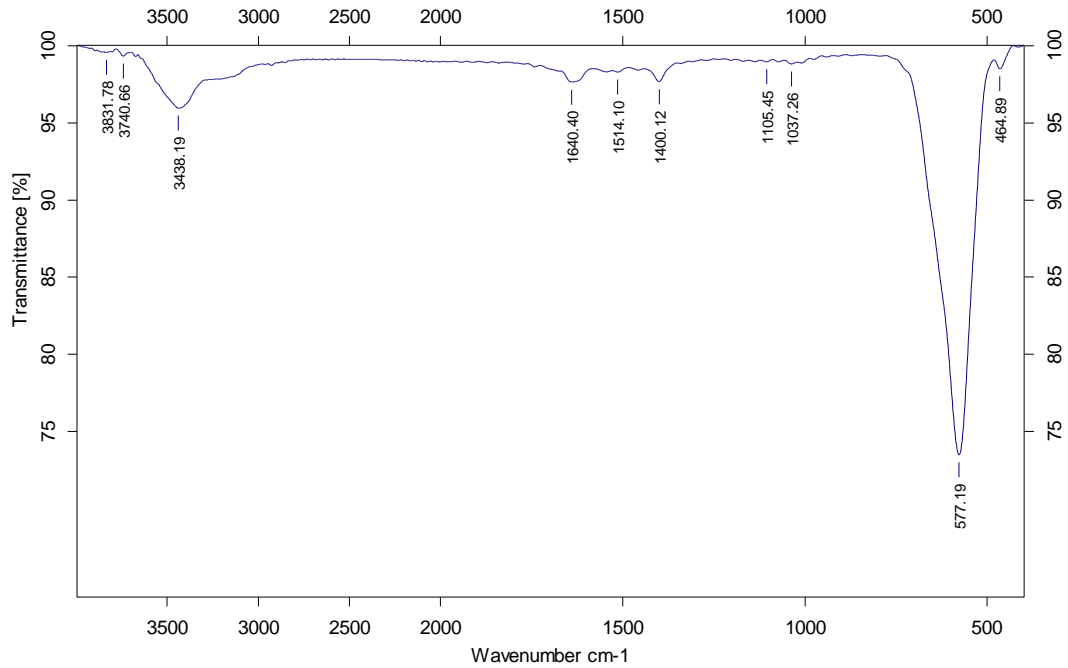
Fig. 2. FT-IR spectrum of nanoparticles of $CuFe_2O_4$ ferrite.

3.3 SEM analysis

The effect of surfactant on the morphology and size of the prepared samples have been studied. Figure 3 shows SEM images of samples prepared using CTAB and SDS as surfactant. The images showed completely agglomerated ferrite particles. It is clearly seen in the micrograph that the sample possess pyramidal nanosize grains. In comparison with other samples, it was observed that the nanoparticles are single crystal, roughly pyramidal and uniformly distributed.
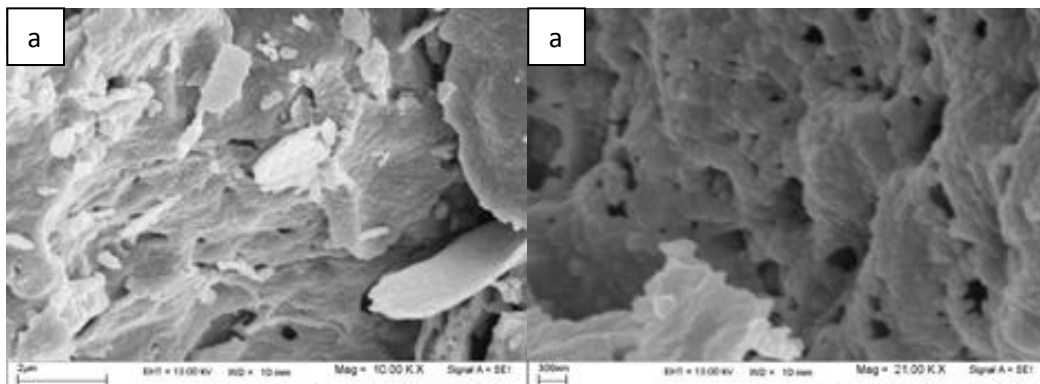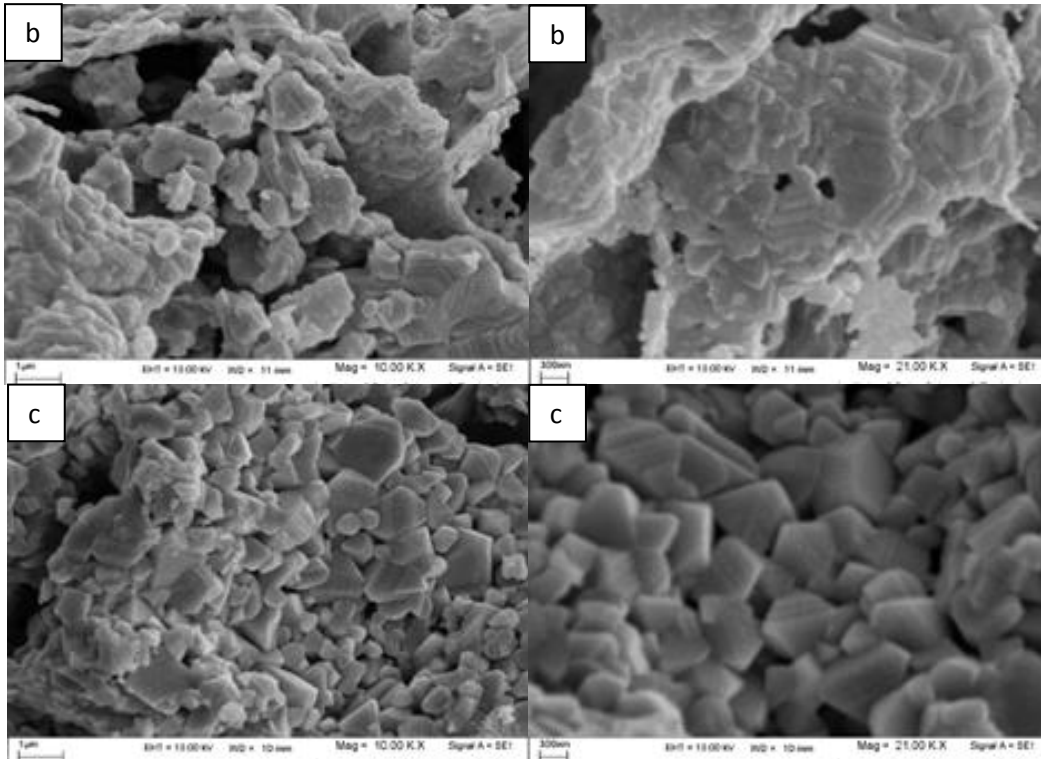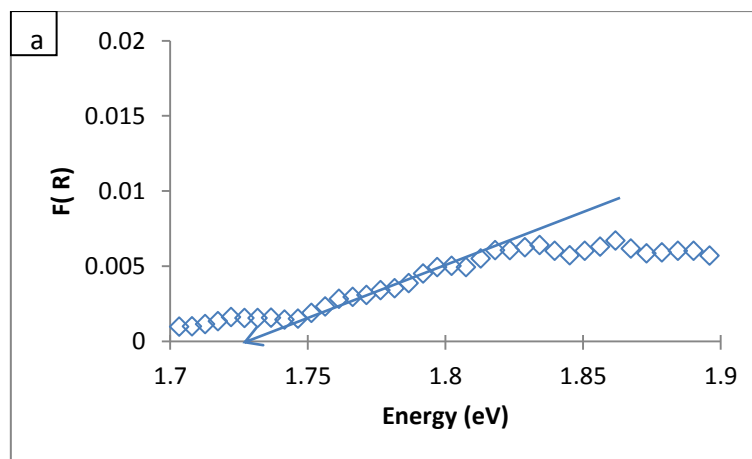
Fig. 3. SEM images: a) CuFe$_2$O$_4$, b) CuFe$_2$O$_4$/CTAB and c) CuFe$_2$O$_4$/SDS.

3.4 DRS analysis

The analysis of optical absorption spectra is a powerful tool for understanding the band structure and band gap of both crystalline and noncrystalline materials. The optical properties of the ferrite samples were characterized by UV-DRS with the help of optical absorption data [16]. Optical band gap of copper ferrite nanoparticles was estimated using the Kubelka-Munk relationship. The Kubelka–Munk plot CuFe$_2$O$_4$, CuFe$_2$O$_4$ using CTAB as surfactant and CuFe$_2$O$_4$ using SDS as surfactant has been presented in Figure 4. The calculated band-gap energies of CuFe$_2$O$_4$, CuFe$_2$O$_4$ using CTAB as surfactant and CuFe$_2$O$_4$ using SDS as surfactant were found to be 1.72, 1.68 and 1.73 eV, respectively.
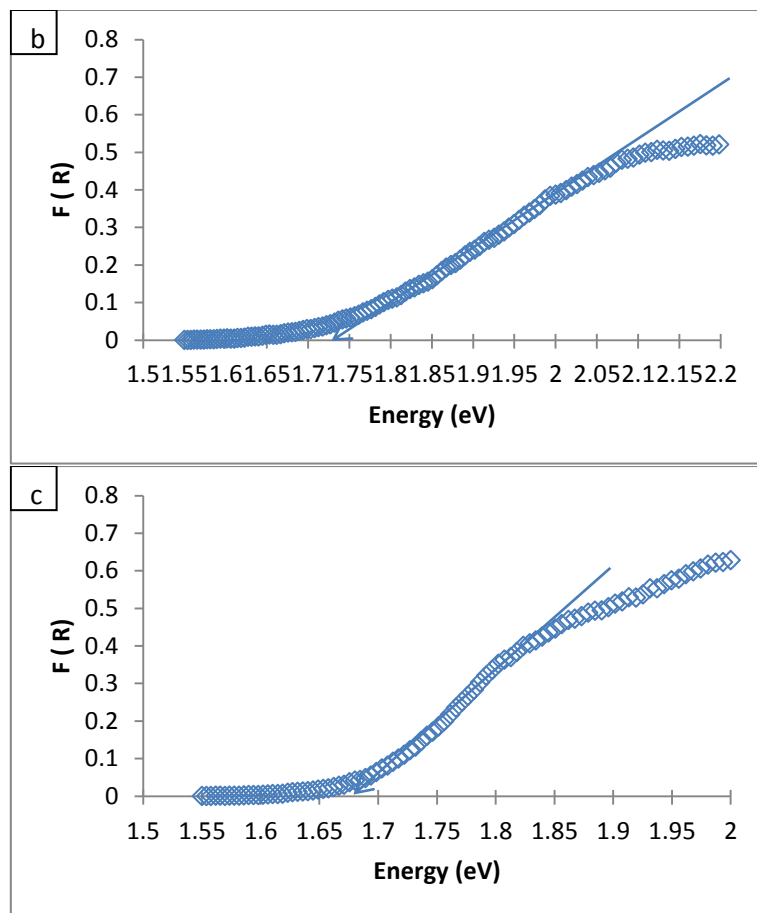
Fig. 4. The Kubelka–Munk plot for a) $CuFe_2O_4$, b) $CuFe_2O_4/CTAB$ and c) $CuFe_2O_4/SDS$.

4. Conclusion

$CuFe_2O_4$, $CuFe_2O_4/CTAB$ and $CuFe_2O_4/SDS$ nanocomposite have been succesfully synthesized by sol-gel auto-combustion method. The nanoparticles were characterized by XRD, SEM, FT-IR and DRS. Powder XRD analysis and FT-IR spectroscopy confirmed formation of $CuFe_2O_4$ spinel phase. The particles size was estimated from SEM data. The energy band gaps were calculated by Kubelka-Munk model from UV−Vis absorption. Applying surfactants along with sol–gel method can improve the properties of the synthesized powders.

References
[1] Y. Shen, Y. Wu, H. Xu, J. Fu, X. Li, Q. Zhao, Y. Hou, Facile preparation of sphere-like copper ferrite nanostructures and their enhanced visible-light-induced photocatalytic conversion of benzene, Materials Research Bulletin, 48 (2013) 4216–4222.
[2] M.M. Rashad, R.M. Mohamed, M.A. Ibrahim, L.F.M. Ismail, E.A. Abdel-Aal, Magnetic and catalytic properties of cubic copper ferrite nanopowders synthesized from secondary resources, Advanced Powder Technology, 23 (2012) 315–323.
[3] M.S. Khandekar, R.C. Kambale, J.Y. Patil, Y.D. Kolekar and S.S. Suryavanshi, Effect of calcination temperature on the structural and electrical properties of cobalt ferrite synthesized by combustion method, Journal of Alloys and Compounds, 509 (2011) 1861–1865.

[4] P. Kumar, S.K. Sharma, M. Knobel and M. Singh, Effect of La^{3+} doping on the electric, dielectric and magnetic properties of cobalt ferrite processed by co-precipitation technique, Journal of Alloys and Compounds, 508 (2011) 115–118.

[5] Y.-D. Xu, G. Wu, H.-L. Su, M. Shi, G.-Y. Yu and L. Wang, Magnetoelectric $CoFe_2O_4$/Pb $(Zr_{0.53}Ti_{0.47})O_3$ composite thin films of 2-2type structure derived by a sol–gel process, Journal of Alloys and Compounds, 12 (2010) 112.

[6] J. Peng, M. Hojamberdiev, Y. Xu, B. Cao, J. Wang and H. Wu, Hydrothermal synthesis and magnetic properties of gadolinium-doped $CoFe_2O_4$ nanoparticles, Journal of Magnetism and Magnetic Materials, 323 (2011) 133–138.

[7] P. Chandramohan, M.P. Srinivasan, S. Velmurugan and S.V. Narasimhan, Cation distribution and particle size effect on Ramanspectrum of $CoFe_2O_4$, Journal of Solid State Chemistry, 184 (2011) 89–96.

[8] J.P. Vejpravova, V. Tyrpekl, S. Danis, D. Niznansky and V. Sechovsky, SSG or SFM state in $CoFe_2O_4$ nano-agglomerates fabricated by micro-emulsion method, Journal of Magnetism and Magnetic Materials, 322 (2010) 1872–1875.

[9] K. Kamal Senapati, C. Borgohain and P. Phukan, Synthesis of highly stable $CoFe_2O_4$ nanoparticles and their use as magnetically separable catalyst for Knoevenagel reaction in aqueous medium, Journal of Molecular Catalysis A: Chemical, 1381 (2011) 3–38.

[10] I.A. Amar, R. Lan, C.T.G. Petit, V. Arrighi and S. Tao, Electrochemical synthesis of ammonia based on a carbonate-oxide composite electrolyte, Solid State Ionics, 182 (2011) 133–138.

[11] B.Y. Song, Y. Eom and T.G. Lee, Removal and recovery of mercury from aqueous solution using magnetic silica nanocomposites, Applied Surface Science, 257 (2011) 4754–4759.

[12] M.S. Khandekar, R.C. Kambale, J.Y. Patil, Y.D. Kolekar, S.S. Suryavanshi, Calcination temperature on the structural and electrical properties of cobalt ferrite synthesized by combustion method, Journal of Alloys and Compounds, 509 (2011) 1861–1865.

[13] W.A.A. Bayoumy, Synthesis and characterization of nano-crystalline Zn-substituted Mg–Ni–Fe–Cr ferrites via surfactant-assisted route, Journal of Molecular Structure, 1056–1057 (2014) 285–291.

[14] A. Pradeep and G. Chandrasekaran, FTIR study of Ni, Cu and Zn substituted nano-particles of $MgFe_2O_4$, Materials Letters, 60 (2006) 371–374.

[15] N.J. Shirtcliffe, S. Thompson, E.S. O'Keefe, S. Appleton and C.C. Perry, Highly aluminium doped barium and strontium ferrite nanoparticles prepared by citrate auto-combustion synthesis, Materials Research Bulletin, 42 (2007) 281–287.

[16] R. Tholkappiyan, K. Vishista, Combustion synthesis of Mg–Er ferrite nanoparticles: Cation distribution and structural, optical, and magnetic properties, Materials Science in Semiconductor Processing, 40 (2015) 631–642.